ELSEVIER

Journal of Hydrology 245 (2001) 48–58

Journal of Hydrology

www.elsevier.com/locate/jhydrol

Soil water content measurements at different scales: accuracy of time domain reflectometry and ground-penetrating radar

J.A. Huisman[a,*], C. Sperl[b], W. Bouten[a], J.M. Verstraten[a]

[a]*Netherlands Centre for Geo-ecological Research (ICG), Institute for Biodiversity and Ecosystem Dynamics (IBED), Physical Geography and Soil Science, Nieuwe Achtergracht 166, 1018 WV Amsterdam, The Netherlands*

[b]*Lehrstuhl für Bodenkunde, TU München, Am Hochanger 2, D-85350 Freising-Weihenstephan, Germany*

Received 14 June 2000; revised 5 November 2000; accepted 30 January 2001

Abstract

Accurate measurements of soil water content with an appropriate support are important in many research fields. Ground-penetrating radar (GPR) is an interesting measurement technique for mapping soil water content at an intermediate scale in between point and remote sensing measurements. To measure soil water content with GPR, we used the velocity of the ground wave, which is the signal traveling directly from source to receiving antenna through the upper centimeters of the soil. To evaluate GPR performance, we aggregated time domain reflectometry (TDR) and gravimetric soil water content measurements to the support of GPR measurements. The results showed that the calibration equations between GPR measurements and aggregated gravimetrical soil water content were similar to those obtained for TDR measurements, suggesting that available TDR calibrations (e.g. Topp's equation) can be used for GPR. Furthermore, we found that the accuracy of GPR to measure soil water content is comparable with the accuracy of TDR, although it depended on the type of data acquisition used for the determination of the ground wave velocity.

Keywords: Ground-penetrating radar; Time domain reflectometry; Soil moisture

1. Introduction

Soil water content is an important variable in hydrological processes at a wide range of scales. At a global scale, soil water content is important because of its interactions with the Earth's climate system. For example, soil water content controls the partitioning of radiation in sensible and latent heat, and couples the soil compartment to the atmosphere in the hydrological cycle by evapotranspiration (Famiglietti et al., 1999). At an intermediate (catchment) scale, the antecedent soil water content (determined by soil type, slope, rainfall distribution etc.) influences the partitioning of precipitation into infiltration and runoff and, therefore, exerts a strong control on soil erosion and flooding (Grayson and Western, 1998). At an even smaller scale, local patterns of soil water infiltration and preferential flow of water in the soil can lead to an accelerated breakthrough of solutes, such as some pesticides and heavy metals, and can, therefore, affect groundwater quality (Ritsema, 1999). In order to cope with these phenomena and to further study the influence of soil water content, there is a need for soil water content measurements at a range of scales.

Available techniques to measure soil water content either provide measurements at a small (point)

* Corresponding author. Tel: +31-20-5257450; fax: +31-20-5257431.

E-mail address: s.huisman@frw.uva.nl (J.A. Huisman).

0022-1694/01/$ - see front matter
PII: S0022-1694(01)00336-5

support (measurement volume) or at the much larger support of remotely sensed data. Time Domain Reflectometry (TDR, Topp et al., 1980) and capacitance measurements (Paltineanu and Starr, 1997) only have a limited support (e.g. 0.01–1 dm^3), which makes them especially useful to measure small-scale processes, such as fingered flow (e.g. Nissen et al., 1999). However, the small support may also mean that many measurements are needed for a reliable areal estimate of soil water content at a larger scale (Western et al., 1998). Neutron probes (Schmugge et al., 1980) do have a larger support (in the order of 0.1–0.5 m^3) but the limited possibilities of automation and multiplexing, as well as the environmental restrictions, hamper estimates of soil water content beyond the support of the neutron probe measurements itself. A promising technique for areal estimates of soil water content over large areas (mapping) is remote sensing, especially passive microwave radiometry (Jackson et al., 1996; Famiglietti et al., 1999). However, many large-scale processes are nonlinearly dependent upon soil water content and, therefore, the spatial variability of soil water content within the radar footprint (ranging from 10 to 1000 m depending on the type of remote sensing) should be better understood to enable an optimal utilization of remotely sensed data.

It can be concluded that there is a gap in support between commonly used field (point) measurements and areal estimates from remote sensing, which gives rise to difficulties because the scale at which the data are collected is not necessarily the scale of practical interest (Western and Blöschl, 1999). One-way to accomplish a 'change to the scale of interest' is within the conceptual framework of spatial aggregation (Heuvelink and Pebesma, 1998; Western and Blöschl, 1999). Another possibility is to focus attention on new techniques to measure soil water content. Ground-penetrating radar (GPR) is one of the promising techniques to measure soil water content at an intermediate scale with supports ranging from 0.5 to 30 m^3 depending on the radar configuration (Du and Rummel, 1994; Chanzy et al., 1996; van Overmeeren et al., 1997; Weiler et al., 1998). The non-invasive character of GPR offers the mobility needed to map soil water content of larger areas (up to 500 × 500 m a day). Furthermore, GPR measures permittivity, just as

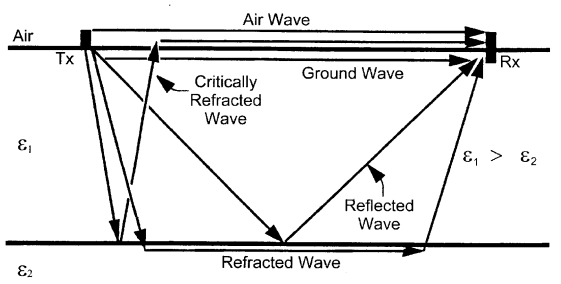

Fig. 1. (after Sperl, 1999): Propagation paths of electromagnetic waves in a soil with two layers of contrasting dielectric permittivity (ϵ_1 and ϵ_2).

TDR and remote sensing, which makes them an attractive triplet to study the spatial structure of soil water content at different scales.

The GPR technique is conceptually quite simple. The essential features are a source antenna placed on the earth surface, radiating energy both upward into the air and downward into the soil, and an antenna receiving the signal transmitted by the source. Any subsurface contrast in electrical properties will result in some energy being reflected back to the surface (Annan, 1973). Fig. 1 shows possible propagation paths in a two-layer soil ($\epsilon_1 > \epsilon_2$). Several of these paths can be used to estimate the permittivity ϵ_1 if the depth to the interface is known (van Overmeeren et al., 1997). For example, Weiler et al. (1998) used the velocity of reflected waves to determine soil permittivity. They proposed a calibration equation relating soil water content to GPR-measured soil permittivity for a Hadley fine sandy loam. They found a small difference between GPR and TDR calibration equations, and this was partly attributed to the difference in frequency range in which TDR and GPR operate and a problem with the determination of the zero offset of the GPR. Unfortunately, the approach of Weiler et al. (1998) cannot be used to map soil water content without extensive boring to determine the depth to the soil interface. Du and Rummel (1994) suggested that without knowledge of soil depth, or in the absence of any (clearly reflecting) soil interface, the ground wave seems to be the most promising wave for mapping soil water content. The ground wave is the signal traveling directly from source to receiving antenna though the upper centimeters of the soil and therefore it is the only wave of which the propagation

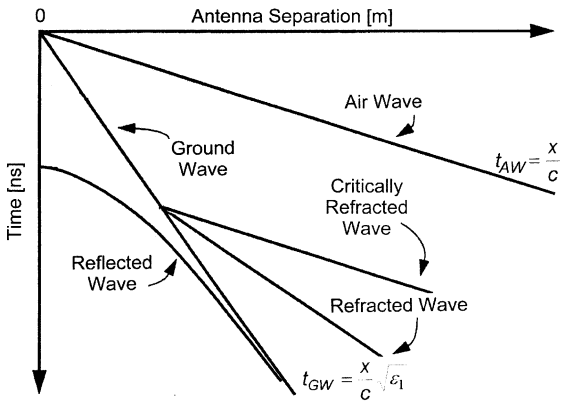

Fig. 2. (after Sperl, 1999): Schematic WARR-measurement. The ground wave can be identified as a wave with a linear move out starting from the origin of the x–t plot.

distance can be known a priori (also see Du, 1996; Sperl, 1999).

The ground wave can be identified in a Wide Angle Reflection and Refraction (WARR) measurement (Figs. 2 and 3). WARR acquisition consists of increasing the distance between the antennae stepwise while one antenna remains at a fixed position. The direct path of the ground wave between source and receiver results in a linear relation between travel time and antenna separation that allows identification of the ground wave. However, the acquisition time of a WARR measurement is long and, consequently, this procedure is impractical for soil water content mapping. It is also possible to determine the ground wave velocity from a radar measurement with a fixed antenna separation (Single Trace Analysis; STA), provided that the ground wave has been identified in a WARR measurement. If this STA approach is accurate enough, the antennae can be placed on sleds, which would provide the mobility to quickly map large areas (Lehmann and Green, 1999).

The aim of this study was (1) to assess the accuracy of GPR to measure soil water content by using the ground wave velocity, and (2) to confirm for a wide array of soils that TDR calibration equations are also valid for GPR. Therefore, we collected TDR, GPR and gravimetric soil water content measurements of the upper 10 cm of the soil on 25 occasions at 13 different sites. The TDR and gravimetric water content measurements were aggregated to the support of GPR, resulting in calibration equations and accuracy assessments for soil water content measurements with TDR and GPR.

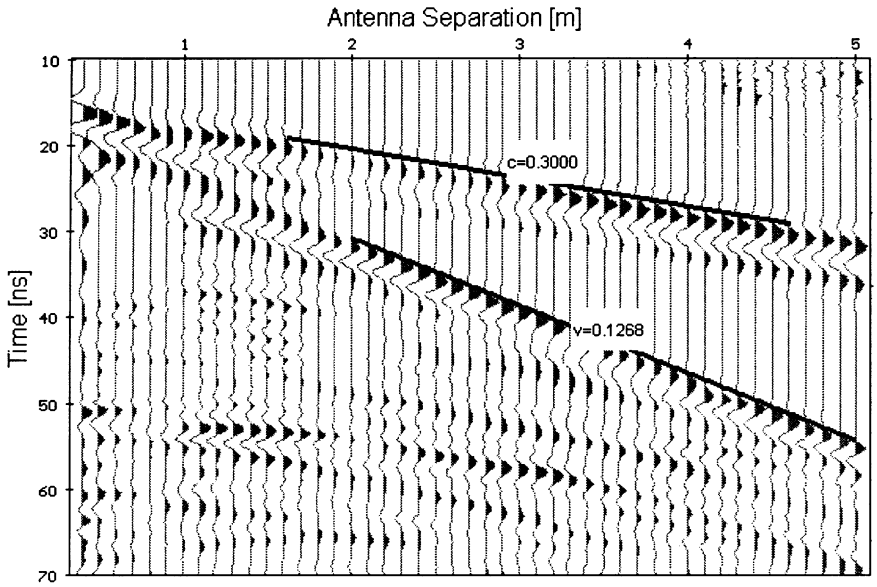

Fig. 3. WARR-measurement recorded in Putten with the 225 MHz antennae. v is the ground wave velocity in mns^{-1}.

2. Materials and methods

Measurements were carried out at 25 measurement locations (from May 1999 to September 1999) at 13 different sites, all located in the Netherlands. The multiple measurements at several sites were not made at the same day. Table 1 summarizes textural properties, textural classes according to the Soil Taxonomy (USDA, 1975), organic matter content, dry bulk density (BD) and the number of visits to each site. Textural properties were obtained with a grain-size analysis of one gravimetric sample per measurement location, and are presented as a weight percentage of the total dry weight of the sample after removal of organic matter. The texture classes range from sand (Kootwijkerzand) to loam (Lelystad). This is a wide array of textures to assess the accuracy of GPR to measure soil water content because high clay contents and the associated high conductivity strongly attenuate the ground wave and, therefore, limit the use of GPR to these lighter textures.

At each of the 25 measurement locations, the permittivity of a $5 \times 2 \times 0.1\ m^3$ plot was estimated by GPR using a WARR measurement along the length axis of the plot (see Fig. 4). In this study, we have (rather arbitrarily) assumed that this plot size corresponds with the support of our GPR measurements. However, recent studies of Sperl (1999) and Wollny (1999) on the 'depth of influence' of the ground wave suggest that the support may well be smaller. Therefore, we will consider errors between assumed and actual GPR support in the following discussions. We used a PulseEKKO™ 1000 GPR system with a 200 V transmitter (Sensors and Software, Mississauga, ON, Canada) and two sets of broadband antennae with center frequencies of 225 and 450 MHz (in air) and frequency bandwidths that are about equal to the center frequency (Davis and Annan, 1989). The radar data were collected with the PulseEKKO™ acquisition software supplied by the manufacturer. The measurements with the 225 MHz antennae were made with antenna separations increasing from 0.4 to 5.0 m with increments of 0.1 m, a time window of 100 ns, a sampling rate of 300 ps and 64 stacks per trace (from 0.3 to 5.0 m with increments of 0.1 m and 100 ps sampling rate in case of the 450 MHz antenna). We used REFLEX (version 4.2, Sandmeier Scientific Software, Karlsruhe, Germany) for standard GPR data processing, including a 'dewow'-filter to remove low-frequency induction effects of the radar equipment, a down trace averaging filter to remove noise and an automatic gain control (AGC) to increase the amplitude of the air and ground wave at large antenna separations.

The average permittivity of each of the $5 \times 2 \times 0.1\ m^3$ plots was also estimated by aggregating 15 randomly located TDR measurements (positions in Fig. 4) collected with a Tektronix cable tester (Tektronix, Beaverton, Oregon, USA) and vertically installed 10 cm long three-wire-probes

Table 1
Textural classes of the 13 soils according to the Soil Taxonomy. %Sand, %Silt and %Clay are expressed as a weight percentage of the total dry weight of the sample after removal of organic matter, OM is the organic matter content expressed in g organic matter per kg dry material, BD is the dry bulk density in kg per dm^3 and N is the number of measurement locations per site

Location	Textural class	%Sand	%Silt	%Clay	OM	BD	N
Muiderberg	Loamy sand	88.0	7.9	4.1	2.0	1.69	2
Lelystad	Loam	29.2	48.4	22.4	7.3	1.25	1
Drie	Loamy sand	80.1	15.9	4.0	4.5	1.38	5
Guttecoven	Silt loam	10.8	75.9	13.4	1.9	1.49	1
Schinveld	Loam	46.6	45.5	7.8	4.1	1.46	1
Koningsbosch	Silt loam	18.4	72.9	8.7	2.4	1.41	1
Mariahoop	Loamy sand	86.3	9.2	4.5	2.2	1.46	1
Echt	Loam	38.0	45.6	16.3	2.8	1.56	1
Elspeet	Loamy sand	82.1	16.7	1.1	6.6	1.18	1
Putten	Loamy sand	83.7	13.7	3.6	5.9	1.44	4
Kootwijk	Loamy sand	87.1	10.4	2.5	4.1	1.51	3
Kootwijkerzand	Sand	98.3	1.1	0.7	0.2	1.62	2
Voorthuizen	Loamy sand	85.1	12.9	2.1	6.7	1.14	2

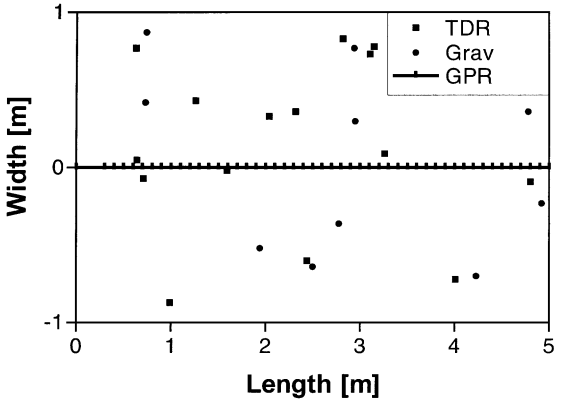

Fig. 4. Sampling locations of TDR, GPR and gravimetric samples within the $5 \times 2 \times 0.1$ m^3 plot.

described by Heimovaara (1993). The Tektronix 1502 series emits a wave packet that has a frequency range 1 MHz to 0.2–1 GHz, depending on the dielectric properties of the soil. The support of these TDR measurements is determined by the length, number, thickness and separation of the probe wires. In case of our three-wire-probes (wire diameter 0.002 m and wire spacing 0.018 m), the support is approximately equal to a cylinder described by the length and the separation of the outer wires (0.03 dm^3), because most energy (>90%) is contained within this volume (Ferré et al., 1998).

Finally, we took 10 vertical gravimetric samples in 0.10 m-length and 0.05 m-diameter stainless steel rings (support of 0.196 dm^3) at randomly selected locations (Fig. 4) at 24 measurement locations (at one location we only took seven samples resulting in a total of 247 gravimetric samples). The gravimetric water content and the dry BD of these samples were determined by measuring the weight loss after 48 h of drying at 70°C. The results were aggregated to estimate the average gravimetric soil water content of each location. In each of the 247 samples we also took TDR measurements to obtain a standard TDR calibration equation.

There are several approaches toward correlating soil water content, θ, with permittivity, but in this paper we choose the semi-theoretical calibration equation of Herkelrath et al. (1991):

$$\theta = b_1 + b_2 n_a, \tag{1}$$

where b_1 and b_2 are calibration parameters, and n_a, the square root of permittivity (also called refractive index) of either GPR or TDR. The TDR refractive index, n_{TDR}, was calculated from the travel time in the soil Δt_s and the length of the probe L according to:

$$n_{TDR} = \frac{c\Delta t_s}{2L} \tag{2}$$

where c is the electromagnetic wave velocity in air (3×10^8 ms^{-1}) and Δt_s was obtained with the travel time analysis presented in Heimovaara and Bouten (1990). For GPR the refractive index was determined using two methods. n_{WARR} was determined by drawing a line parallel with the arrival times of the ground wave in a limited window of antenna separations (see Fig. 3). The lower limit of this window was determined by the amount of interference between air and ground wave at short separations, whereas the upper limit depended on the ground wave attenuation with increasing antenna separation. In the STA, the refractive index, n_{STA}, was calculated from the arrival time of the air wave and the ground wave at a specific antenna separation x:

$$n_{STA} = \frac{c(t_{GW} - t_{AW}) + x}{x}, \tag{3}$$

where t_{GW} and t_{AW} are the arrival times of the ground wave and the air wave, respectively. The arrival times can be determined manually or semi-automatically with a time picking algorithm often available in seismic or GPR data processing packages (see e.g. Molyneux and Schmitt, 1999). We used REFLEX for both the WARR analysis and the manual picking of arrival times in the STA. The traces needed for the STA were extracted from the WARR measurement. Consequently, we do not consider the uncertainty associated with the proper identification of the ground wave in a single trace.

To quantify the accuracy of the calibration between soil water content and refractive index, we used the root mean square error (RMSE) between observed water content, θ_{obs}, and water content predicted by the calibration Eq. (1), θ_{est}

$$RMSE = \sqrt{\frac{\sum_{i=1}^{N} (\theta_{obs} - \theta_{est})^2}{N}} \tag{4}$$

where N is the number of observations. However, in case of scarce data this can lead to an overestimation of accuracy because of (a) overfitting due to overparametrization and (b) neglecting uncertainty in estimation of the regression coefficients. Therefore, we fitted only part of the available data (60%) with Eq. (1). The validation set (consisting of the remaining 40% of the data) was used to obtain a better estimate of the accuracy of the soil water content measurements, again expressed by the RMSE. The random separation in calibration and validation sets was repeated 1000 times to reduce the influence of atypical sets on the results.

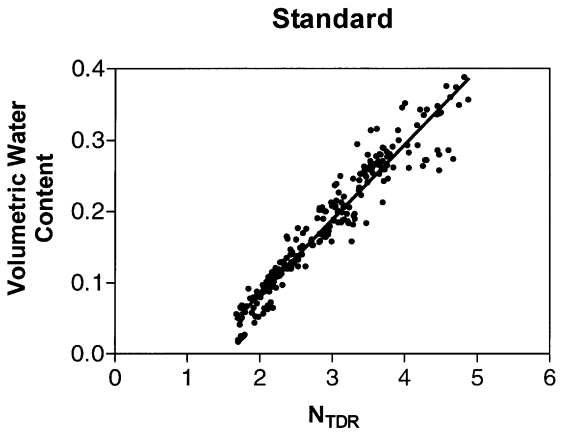

Fig. 5. Standard calibration equation between volumetric water content and refractive index n_{TDR} (247 samples).

3. Results and discussion

3.1. Aggregation of TDR measurements

Figure 5 presents the standard calibration equation between n_{TDR} and θ (also see Table 2). Close inspection reveals several clusters of measurements, each corresponding with a measurement location. The RMSE of this TDR calibration equation is 0.0243 $m^3\ m^{-3}$ (average RMSE of 1000 validation sets), which is close to the average RMSE of the calibration sets because there are sufficient data to accurately estimate the regression coefficients. Both the calibration equation and its accuracy are within the range found by others (e.g. Jacobsen and Schjønning, 1994).

The calibration equation resulting from the aggregation of the TDR measurements and the gravimetrical water contents for each of the 25 measurement locations is shown in Fig. 6. It is clear that aggregation did not greatly affect the calibration equation (Table 2). The average RMSE of the aggregated soil water content estimation was 0.0305 $m^3\ m^{-3}$ for the validation sets, which is higher than the RMSE of the calibration sets due to the uncertainty in the estimation of the regression coefficients. Generally, the RMSE of aggregated TDR measurements can be separated in several error sources: (A) uncertainty in aggregation of n_{TDR} and θ, (B) measurement error in n_{TDR}, (C) measurement error in θ, and (D) model error in $\theta - n_{TDR}$ relationship. The error bars in Fig. 6 represent the standard error of the mean (15 TDR measurements and 10 gravimetric samples) and because they are small, it can be concluded that the errors A to C are small compared to error D, the model error. Of course, this is already well established for standard TDR calibrations and can be illustrated by including more parameters affecting permittivity in the calibration

Table 2
Regression parameters relating soil water content to refractive index. Mean and standard deviations (in parentheses) of 1000 randomly selected combinations of validation and calibration sets. N is the size of the calibration set

	b_1	b_2	RMSE (calibration)	RMSE (validation)	N
TDR (Standard)	−0.1263 (0.0051)	0.1049 (0.0019)	0.0239 (0.0011)	0.0243 (0.0018)	150
TDR (Aggregated)	−0.1510 (0.0162)	0.1082 (0.0063)	0.0269 (0.0053)	0.0305 (0.0071)	15
GPR (WARR, 225 MHz)	−0.1732 (0.0201)	0.1147 (0.0068)	0.0241 (0.0042)	0.0281 (0.0065)	15
GPR (WARR, 450 MHz)	−0.1564 (0.0227)	0.1088 (0.0076)	0.0266 (0.0026)	0.0308 (0.0048)	15
GPR (STA, 225 MHz)[a]	−0.1499 (0.0195)	0.1082 (0.0063)	0.0338 (0.0055)	0.0376 (0.0085)	15

[a] STA = Single trace analysis.

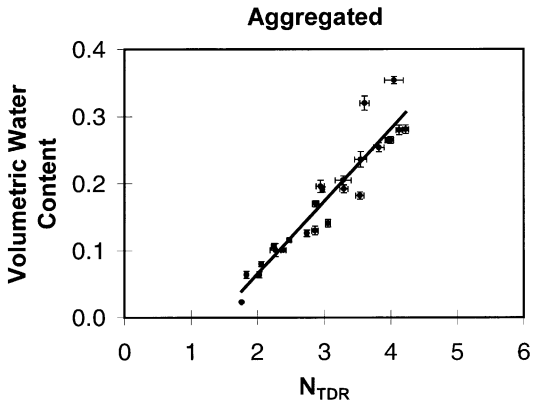

Fig. 6. Aggregated calibration equation between average volumetric water content and average refractive index n_{TDR} for 25 measurement locations.

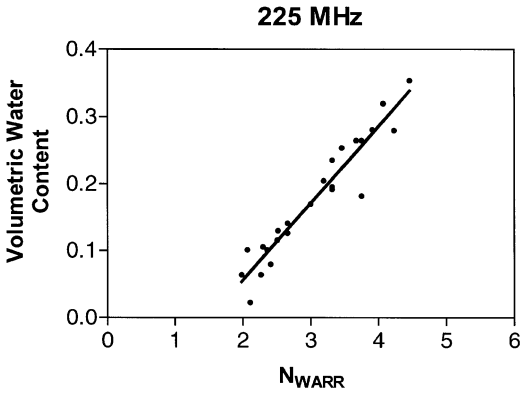

Fig. 7. Calibration equation between volumetric water content and refractive index n_{WARR} obtained with 225 MHz antennae (24 locations because one location could not be sampled with the 225 MHz antennae due to furrows).

(e.g. Ledieu et al., 1986; Malicki et al., 1996). In this study, the addition of BD:

$$\theta = b_3 + b_4 n_{TDR} + b_5 BD \quad (5)$$

gave a significant decrease of RMSE to 0.0210 $m^3\ m^{-3}$ before aggregation and a decrease to 0.0262 $m^3\ m^{-3}$ after aggregation (Table 3). In contrast to previous studies, such as Ledieu et al. (1986), the intercepts (b_3) of our calibration equations did not significantly deviate from zero, and were, therefore, omitted from the calibration. Estimates of %sand, %silt, %clay and organic matter content were also available (one sample for each measurement location), but the inclusion of these parameters did not significantly improve the estimation of soil water content.

3.2. Accuracy of soil water content measurements with GPR (WARR measurement)

Figure 3 shows a typical WARR measurement measured with the 225 MHz antennae. Both the air wave and the ground wave can easily be recognized due to their linear move out with increasing antenna separation. The ground wave velocity is 0.1268 m ns^{-1}, which corresponds with a refractive index of 2.37 (and a permittivity of 5.60). For comparison, the aggregated refractive index of the TDR measurements was 2.26 and the aggregated gravimetric soil water content was 0.010 $m^3\ m^{-3}$. For this WARR measurement, the range of antenna separations at which the ground wave can be recognized runs from 1.2 to 5.0 m.

The calibration equation between aggregated soil water content and n_{WARR} (225 MHz antennae) is shown in Fig. 7 and the results for 225 and 450 MHz are summarized in Table 2. The similarity between Figs. 6 and 7 and the calibration equations

Table 3
Regression parameters relating soil water content to refractive index and dry BD. Mean and standard deviations (in parentheses) of 1000 randomly selected combinations of validation and calibration sets. N is the size of the calibration set

	b_4	b_5	RMSE (calibration)	RMSE (validation)	N
TDR (Standard)	0.1013 (0.0013)	− 0.0804 (0.0022)	0.0208 (0.0008)	0.0210 (0.0017)	150
TDR (Aggregated)	0.1061 (0.0065)	− 0.1010 (0.0129)	0.0219 (0.0033)	0.0262 (0.0052)	15
GPR (WARR, 225 MHz)	0.1087 (0.0039)	− 0.1076 (0.0086)	0.0215 (0.0027)	0.0241 (0.0046)	15
GPR (WARR, 450 MHz)	0.1059 (0.0051)	− 0.1027 (0.0107)	0.0216 (0.0018)	0.0250 (0.0034)	15
GPR (STA, 225 MHz)[a]	0.1016 (0.0046)	− 0.0902 (0.0104)	0.0329 (0.0055)	0.0361 (0.0089)	15

[a] STA = Single trace analysis.

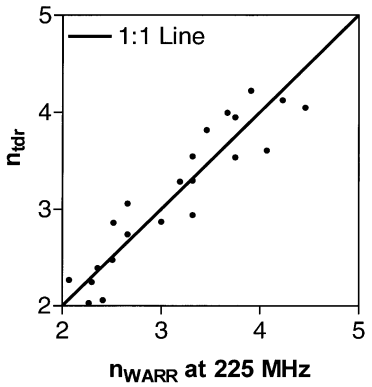

Fig. 8. Comparison of n_{TDR} and n_{WARR} (225 MHz).

presented in Table 2 suggest a close agreement between GPR and TDR measurements despite the different operating frequencies of both methods. Contrary to the results of Weiler et al. (1998) based on the velocity of reflected waves, we did not find a structural difference between GPR and TDR calibration equations based on ground wave velocity. The RMSE of the soil water content estimation with n_{WARR} was 0.0281 $m^3\,m^{-3}$, in the case of the 225 MHz antennae, and 0.0308 $m^3\,m^{-3}$ in the case of the 450 MHz antennae. This is comparable with the accuracy of TDR, which was 0.0305 $m^3\,m^{-3}$. The RMSE of GPR was reduced to 0.0250 $m^3\,m^{-3}$ by including dry BD in the calibration, which is a similar reduction to that in TDR (Table 3). Generally, there is an excellent agreement between GPR and TDR, as shown in Fig. 8. This suggests that the ground wave velocity adequately represents the upper 10 cm of the soil (length of TDR probe!), relatively independent of the antenna frequency f and the permittivity ϵ_r (Figs. 8 and 9b). This seems to contradict the traditional assumption that the depth of influence of the ground wave is linearly proportional to the wavelength ($\lambda = c/(f\sqrt{\epsilon_r})$, ranging from 0.10–0.70 m in this study), but it could just as well indicate a homogeneous permittivity profile in the topsoil at our measurement locations.

As with TDR, it is illustrative to separate the error in the soil water content measurements with GPR in several sources: (A) error in n_{WARR} (e.g. reproducibility of GPR wave trace, reproducibility of WARR measurement and analysis), (B) uncertainty in aggregation and measurement error in θ (same as in TDR error analysis), (C) model error in $\theta - n_{WARR}$ relationship and (D) mismatch between aggregated support of θ ($5 \times 2 \times 0.1$ m^3) and the actual (ill-defined) support of GPR. The similarity between the calibration of TDR and GPR suggests that the model error should be dominant for both methods. However, this should have led to a substantial decrease in scatter when the permittivity of TDR and GPR are compared directly (Fig. 8), which seems not to be the case. Besides the model error, the RMSE of GPR must, therefore, at least partly be explained by (A) errors in n_{WARR} or (D) mismatch in sample volumes. These two sources of error are not readily separated in this study, but some tentative results can be extracted from Fig. 9. Figure 9a compares WARR measurements made in opposite directions at all measurement locations and indicates that the GPR measurements are highly reproducible at low permittivity, whereas at higher permittivities the difference between two WARR measurements in opposite directions increase. A possible explanation for this could be that the mismatch between the actual and assumed support of the WARR measurement increased (for example due to the fact that the ground wave was not present at large antenna separations in wet soils, as was the case in this study). Fig. 9b compares WARR measurements made with different antenna frequencies, but in the same direction, and, again, the deviations increase with increasing permittivity. The similarity between Fig. 9a and b suggests that the decrease in reproducibility shown in Fig. 9a is mainly caused by an increase of error in n_{WARR}, and not by the increasing mismatch in sample volume. The increasing error in n_{WARR} can be understood when the propagation of velocity errors into the determination of n_{WARR} is considered. If we assume a constant velocity error Δv, which is reasonable in the case of the 'tangent line' analysis used to analyze the WARR measurements, then the error in refractive index Δn_{WARR} can be calculated according to:

$$\Delta n_{WARR} = \frac{1}{2}(n_{WARR,max} - n_{WARR,min}) = \frac{1}{2}\left(\frac{c}{v - \Delta v} - \frac{c}{v + \Delta v}\right) = \frac{c\Delta v}{v^2 - (\Delta v)^2}. \quad (6)$$

From Eq. (6) it can be seen that Δn_{WARR} increases with

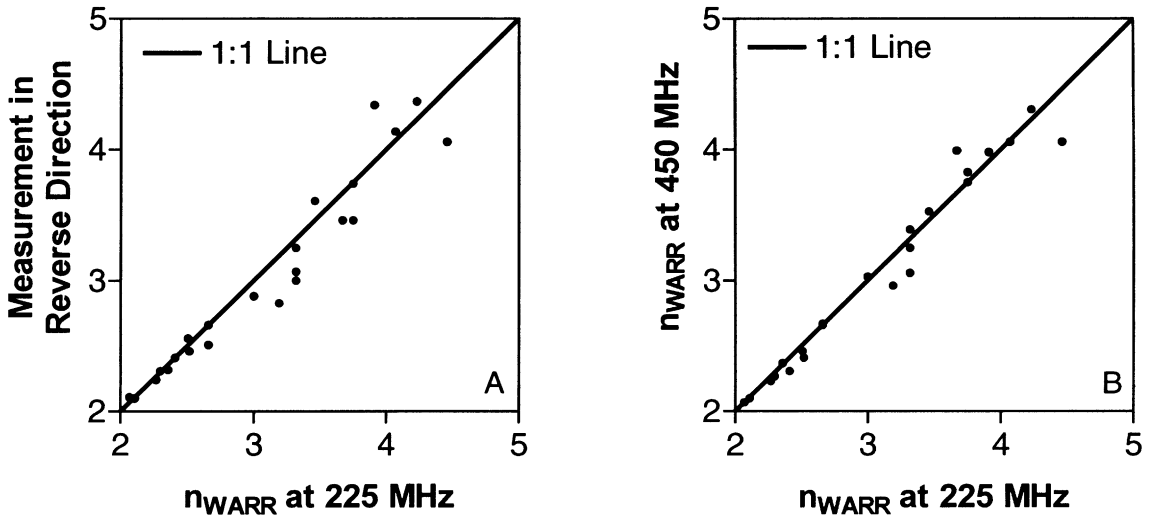

Fig. 9. (a) Comparison of n_{WARR} (225 MHz) measured in opposite directions, (b) Comparison of n_{WARR} (225 MHz) and n_{WARR} (450 MHz) measured in the same direction.

lower velocity v, and therefore increases with n_{WARR}. For example, if we assume that $\Delta v = 0.005$ m ns^{-1} then Δn_{WARR} is 0.067 for $n_{WARR} = 2$ and 0.420 for $n_{WARR} = 5$.

3.3. Accuracy of soil water content measurements with GPR (STA)

The results of the STA are also presented in Tables 2 and 3. The traces used in the STA were selected directly from the WARR measurements. The antenna separation of the selected trace depended on the recognizability of the ground wave, and varied from 1.4 to 2.9 m with a median of 2.5 m. Again, the results obtained with GPR compare well with the calibration equation obtained for TDR in terms of slope and intercept. The RMSE of the soil water content measurements with the STA increased compared with the RMSE of the WARR measurement. Possible extra sources of error are (A) the mismatch between the assumed ($5 \times 2 \times 0.1$ m^3) and the actual support in the STA (dependent on fixed antenna separation) and (B) the uncertainty involved with the estimation of the ground wave velocity from one trace, which can be separated in (B1) errors associated with the position of the antennae and (B2) errors associated with the picking of the arrival times. The positional error is also present in WARR measurements, but the analysis of these measurements is not sensitive to errors in individual traces because these are averaged out in the 'global' analysis.

The mismatch between the assumed and the actual support is obvious in case of the STA because the spatial averaging is restricted to the chosen (fixed) antenna separation. However, the traces used in the STA were extracted from the WARR measurements, and for these measurements it was already concluded that support mismatches are not a major source of error. Therefore, the error in n_{STA} (B1 and B2) seems to be responsible for the increase in error with respect to the WARR measurements and the TDR measurements. With respect to future application of the STA to soil water content mapping, this suggests that an increase of accuracy can easily be achieved by averaging the permittivity estimates from several 'single traces'.

4. Conclusions

We evaluated the accuracy of GPR and TDR to measure and map volumetric soil water content. We focused on the velocity of the ground wave (at different antennae frequencies), which can be determined from a WARR measurement. However, to allow mapping of soil water content over large areas, we

also considered a simplified acquisition based on the analysis of a single trace acquired with a fixed antenna separation (STA).

The accuracy of TDR, WARR measurements and the STA to measure soil water content was determined from calibration equations between aggregated soil water content and refractive index. The main error source in the aggregated TDR calibration equation was the model error between water content and refractive index, which provides an upper limit on the accuracy of soil water content measurements with electromagnetic methods (in the case of our aggregated TDR measurements, the accuracy was $\pm 0.030\ m^3\ m^{-3}$, although accuracy did improve by including more soil physical properties). The dominance of the model error suggests that the most meaningful comparison of different electromagnetic methods is based on permittivity, and not on soil water content. The calibration equation based on the WARR measurements compared well with the TDR calibration equation, and the accuracy of soil water content measurements with WARR measurements was $\pm 0.030\ m^3\ m^{-3}$. The error in soil water content measurements with WARR measurements was partly attributed to the uncertainty in the velocity determination, which mainly affected the accuracy of soil water content measurements in wet soils. The accuracy of the soil water content measurements with the STA was $\pm 0.037\ m^3\ m^{-3}$. The increase in error from the WARR measurements to the STA was mainly attributed to an increase in error of the velocity determination. Therefore, it seems possible to decrease the error of the STA by using several 'single traces' or a GPR with multiple receivers to determine ground wave velocity.

Generally, the good correspondence between TDR and GPR confirms that available TDR calibrations between soil water content and permittivity, such as a site-specific calibration equation or Topp's equation, can be used directly for soil water content measurements with GPR for a wide array of textures ranging from sand to loam. GPR is less likely to be successful for heavier textures because the high conductivity of these soils generally results in a strong attenuation of the ground wave, which makes the identification of the ground wave and the subsequent determination of the ground wave velocity hard to impossible. Altogether, GPR seems a promising technique for accurate soil water content measurements over large areas.

Acknowledgements

NWO-ALW grant number 750-19-804 financially supported this study. S.C Dekker, B. Jansen, M. van der Gulik, M.T. van Wijk and L. de Lange are thanked for assistance during the fieldwork period. The constructive comments of the reviewers improved the quality of this paper.

References

Annan, A.P., 1973. Radio interferometry depth sounding: part I — theoretical discussion. Geophysics 38 (3), 557–580.

Chanzy, A., Tarussov, A., Judge, A., Bonn, F., 1996. Soil water content determination using a digital ground-penetrating radar. Soil Science Society of America Journal 60, 1318–1326.

Davis, J.L., Annan, A.P., 1989. Ground-penetrating radar for high resolution mapping of soil and rock stratigraphy. Geophysical Prospecting 37, 531–551.

Du, S., 1996. Determination of water content in the subsurface with the ground wave of ground penetrating radar. Ludwig-Maximilians-Universität, München, p. 117.

Du, S., Rummel, P., 1994. Reconnaissance studies of moisture in the subsurface with GPR. In: Fifth international conference on ground penetrating radar. Waterloo Center for Groundwater Research, Waterloo, Kitchener, Ontario, Canada, pp. 1241–1248.

Famiglietti, J.S., et al., 1999. Ground-based investigation of soil moisture variability within remote sensing footprints during the Southern Great Plains 1997 (SGP97) hydrology experiment. Water Resources Research 35 (6), 1839–1851.

Ferré, P.A., Knight, J.H., Rudolph, D.L., Kachanoski, R.G., 1998. The sample areas of conventional and alternative time domain reflectometry probes. Water Resources Research 34 (11), 2971–2979.

Grayson, R.B., Western, A.W., 1998. Towards areal estimation of soil water content from point measurements: time and space stability of mean response. Journal of Hydrology 207, 68–82.

Heimovaara, T.J., 1993. Design of triple-wire time domain reflectometry probes in practice and theory. Soil Science Society of America Journal 57, 1410–1417.

Heimovaara, T.J., Bouten, W., 1990. A computer-controlled 36-channel time domain reflectometry system for monitoring soil water contents. Water Resources Research 26 (10), 2311–2316.

Herkelrath, W.N., Hamburg, S.P., Murphy, F., 1991. Automatic, real time monitoring of soil moisture in a remote field area with time domain reflectometry. Water Resources Research 22 (5), 857–864.

Heuvelink, G.B.M., Pebesma, E.J., 1998. Spatial aggregation and soil process modeling. Geoderma 89 (1–2), 47–65.

Jackson, T.J., Schmugge, J., Engman, E.T., 1996. Remote sensing applications to hydrology: soil moisture. Hydrological Sciences Journal 41 (4), 517–530.

Jacobsen, O.H., Schjønning, P., 1994. Comparison of TDR calibration functions for soil water determination. In: Jacobsen, O.H., Petersen, L.W. (Eds.), Time-domain reflectometry, applications in soil science. SP report. Danish Inst. of Plant and Soil Science, Research Center Foulum, Denmark, pp. 25–33.

Ledieu, J., De Ridder, P., De Clerck, P., Dautrebande, S., 1986. A method of measuring soil moisture by time domain reflectometry. Journal of Hydrology 88, 319–328.

Lehmann, F., Green, A.G., 1999. Semiautomated georadar data acquisition in three dimensions. Geophysics 64 (3), 719–731.

Malicki, M.A., Plagge, R., Roth, C.H., 1996. Improving the calibration of dielectric TDR soil moisture determination taking into account the solid soil. European Journal of Soil Science 47, 357–366.

Molyneux, J.B., Schmitt, D.R., 1999. First-break timing: arrival onset times by direct correlation. Geophysics 64 (5), 1492–1501.

Nissen, H.H., Moldrup, P., de Jonge, L.W., Jacobsen, O.H., 1999. Time Domain Reflectometry coil probe measurements of water content during fingered flow. Soil Science Society of America Journal 63, 493–500.

van Overmeeren, R.A., Sariowan, S.V., Gehrels, J.C., 1997. Ground penetrating radar for determining volumetric soil water content; results of comparative measurements at two sites. Journal of Hydrology 197, 316–338.

Paltineanu, I.C., Starr, J.L., 1997. Real-time soil water dynamics using multisensor capacitance probes: laboratory calibration. Soil Science Society of America Journal 61, 1576–1585.

Ritsema, C.J., 1999. Special issue: preferential flow of water and solutes in soils. Journal of Hydrology 215, 1–3.

Schmugge, T.J., Jackson, T.J., McKim, H.L., 1980. Survey of methods for soil moisture determination. Water Resources Research 16 (6), 961–979.

Sperl, C., 1999. Erfassung der raum-zeitlichen Variation des Bodenwassergehaltes in einem Agrarökosystem mit dem Ground-Penetrating Radar. Technische Universität München, München, p. 182.

Topp, G.C., Davis, J.L., Annan, A.P., 1980. Electromagnetic determination of soil water content: measurements in coaxial transmission lines. Water Resources Research 16 (3), 574–582.

USDA, 1975. Soil Taxonomy: a basic system of soil classification for making and interpreting soil surveys. Agric. Handbook 436, USDA (United States Department of Agriculture) Soil Conservation Service, Washington D.C., USA.

Weiler, K.W., Steenhuis, T.S., Boll, J., Kung, K.-J.S., 1998. Comparison of ground penetrating radar and time domain reflectometry as soil water sensors. Soil Science Society of America Journal 62, 1237–1239.

Western, A.W., Blöschl, G., 1999. On the spatial scaling of soil moisture. Journal of Hydrology 217, 203–224.

Western, A.W., Blöschl, G., Grayson, R.B., 1998. Geostatistical characterisation of soil moisture patterns in the Tarrawarra catchment. Journal of Hydrology 205, 20–37.

Wollny, K.G., 1999. Die Natur der Bodenwelle des Georadar und ihr Einsatz zur Feuchtebestimmung. Ludwig-Maximilians-Universität, München, p. 169.